# Deactivation of zeolite catalyst H-ZSM-5 during conversion of methanol to gasoline: operando time and space resolved X-ray diffraction

*Daniel Rojo-Gama[a,b], Lukasz Mentel[a], Georgios N. Kalantzopoulos[a], Dimitrios K. Pappas[a], Iurii Dovgaliuk[c], Unni Olsbye[a], Karl Petter Lillerud[a], Pablo Beato[b], Lars F. Lundegaard*[b], David S. Wragg[a] and Stian Svelle*[a]*

[a] Center for Materials Science and Nanotechnology (SMN), Department of Chemistry, University of Oslo, P.O. Box 1033, Blindern, N-0315 Oslo, Norway

[b] Haldor Topsøe A/S, Haldor Topsøes Allé 1, 2800 Kgs. Lyngby, Denmark

[c] Swiss-Norwegian Beamline, The European Synchrotron, European Synchrotron Radiation Facility 6, Rue Jules Horowitz, 38000 Grenoble (France)

**Corresponding Author**

- Prof. Stian Svelle: stian.svelle@kjemi.uio.no

- Dr. Lars F. Lundegaard: lafl@topsoe.com

The deactivation of zeolite catalyst H-ZSM-5 by coking during the conversion of methanol to hydrocarbons was monitored by high energy space- and time- resolved operando X-ray diffraction. Space resolution was achieved by continuous scanning along the axial length of a capillary fixed bed reactor with a time resolution of 10 seconds per scan. Using real structural parameters obtained from the XRD we can track the development of coke at different points in the reactor and link this to a kinetic model to correlate catalyst deactivation with structural changes occurring in the material. The “burning cigar” model of catalyst bed deactivation is directly observed in real time.

**TOC GRAPHICS**

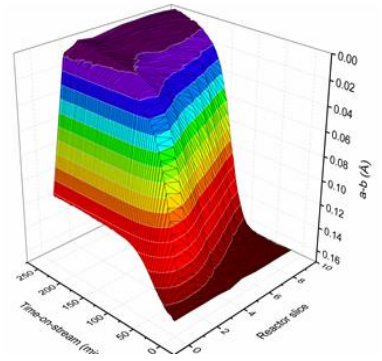


**KEYWORDS** Coke, Heterogeneous catalysis, Methanol-to-Hydrocarbons, Time-resolved, X-Ray Diffraction , Zeolites

To monitor, to fundamentally understand, and ideally to control catalyst deactivation by coking are high priority issues of immediate industrial importance. In this contribution, we resolve the first issue and make significant progress towards the second for the conversion of methanol to hydrocarbons over zeolite catalyst H-ZSM-5[1-2]; thereby providing tools to tackle the third. Catalyst deactivation by carbon deposition or coking is a major limiting issue in many petrochemical and refining processes that rely on heterogeneous catalysis. It necessitates catalyst regeneration[3-4] and/or replacement, increasing plant complexity and reducing productivity. This translates to increased production costs and environmental impact. H-ZSM-5 is employed commercially for the conversion of methanol to propene (MTP) and gasoline (MTG). Nevertheless, these processes still suffer from deactivation and reactor down time, in practice resulting in the need for an extra "swing" reactor. Mobil's original New Zealand MTG plant had 4 reactors producing gasoline and one undergoing regeneration at any point in time[5].

In key studies from Haw and co-workers for SAPO-34 (another industrial methanol conversion catalyst selective for ethene and propene)[6] and Schulz for H-ZSM-5[4], it has been demonstrated that for fixed bed reactors, the type of reactor industrially applied, the deactivation occurs gradually from the inlet to the outlet, referred to as "the burning cigar"[6]. In recent contributions, ex-situ analysis based on the physical separation of deactivated zeolite catalyst beds have shown that on medium pore size zeolites the deactivation does indeed occur from inlet to outlet[7-9]. However, for large pore size zeolites such as Mordenite and Beta the deactivation appears to take place more homogeneously throughout the bed [7].

X-ray based techniques employing synchrotron radiation have been proven to be very useful for monitoring chemical reactors[10]. As reviewed by Beale et al.[11], much progress has been made in the imaging of functional materials under the conditions typically used in a real industrial

process. Of particular relevance here, are two studies utilizing similar methodologies to monitor the catalyst during the conversion of methanol over SAPO-34[12-13]. By moving the reactor repeatedly in the X-ray beam (a z-axis scan or z-scan), spatiotemporal variations in the reactor related to both the induction period and the deactivation of the catalyst were found[13]. However, later attempts extend these studies to H-ZSM-5[14] proved less insightful, revealing only very subtle changes during the process, whereas similar investigations of the unidimensional 10-ring zeolite H-ZSM-22[15] revealed that the expansion of the unit cell matched activity gradients in the reactor. In a recent study of H-ZSM-5 relying on cumbersome ex situ methods, we were able to demonstrate that that the unit cell of the crystalline catalyst changes upon deactivation, at both atmospheric and elevated reaction pressure. We were able to establish a correlation between these changes and classical deactivation parameters, such as the total amount of coke, the remaining acidity, and the remaining surface area[16]. However, the extent to which these observations, made "post mortem" can be transferred to the working catalyst needs clarification.

In this study, the MTG reaction has been monitored with time and space resolved X-ray diffraction over H-ZSM-5 using a capillary fixed bed reactor. A commercial H-ZSM-5 catalyst with high Al content, in contrast to previous studies[14] has been used, to achieve and maintain full initial methanol conversion for a prolonged period yet without making the experiment too extensive. Basic characterization of the catalyst can be found in the Supporting Information (S.I.). Data were acquired by repeatedly scanning the X-ray beam along the length of a capillary reactor (z-scan) which was under a continuous feed of reactants. The experiment was performed on the Swiss-Norwegian beamline (BM01) at the European Synchrotron Facility (ESRF). In addition, the product stream was analyzed on-line by mass spectrometry. Further experimental details are provided in the Methods section and in the S.I. Armed with the insights from the ex

situ study[16], we here utilize the direct correlation between the structure of H-ZSM-5 (more specifically the difference between the length of the a- and b-axes of the unit cell) and the degree of deactivation. Due to the high signal to noise ratio, excellent peak resolution, and rapid acquisition time of the X-ray diffractograms, we have been able, using parametric Rietveld analysis, to follow the evolution of the crystal structure for the different positions of the bed at increasing reaction times during the deactivation of the catalyst.

Photographs of the catalyst bed before, during and after the MTH reaction are provided in Figure 1.

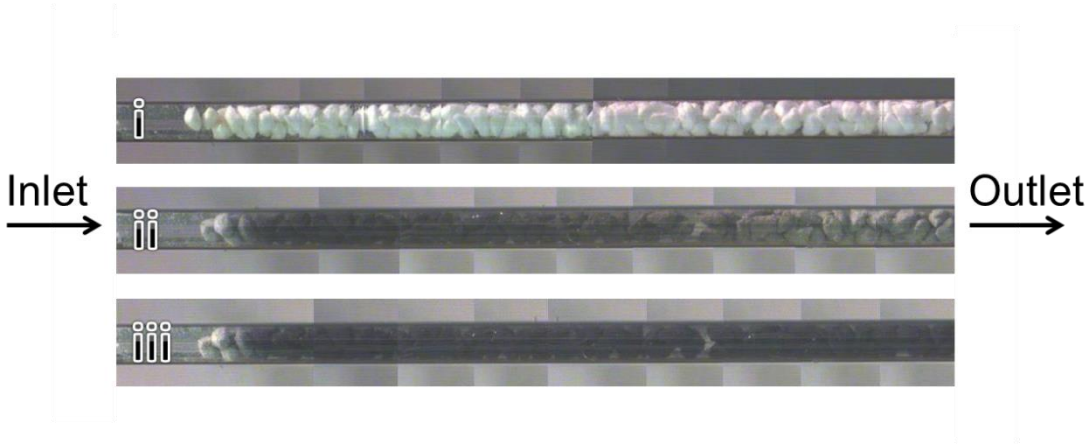


**Figure 1.** Photographs of the catalyst bed taken with the alignment camera for (i) the activated, fresh catalyst sample, (ii) after 75 min on stream, and (iii) for the completely deactivated catalyst. Reaction at WHSV = 20 gMeOH gcat-1 h-1 and 400 °C.

Clearly, the coking, reflected by the intensity of the black color, progresses gradually from the inlet to the outlet. In parallel, the reaction front moves from the inlet towards the outlet of the reactor during the reaction, as described in previous MTH studies over H-ZSM-5 [4, 7, 17]. A white layer of catalyst at the very inlet of the reactor is seen even for the completely deactivated sample. This is due to the initial build up of hydrocarbon pool species and is evident here

because of the high feed rate/linear gas velocity achieved in the very narrow capillary (see below)[18].

The different panels of Figure 2 highlight the key changes in the diffractogram of H-ZSM-5 with the progress of the reaction.

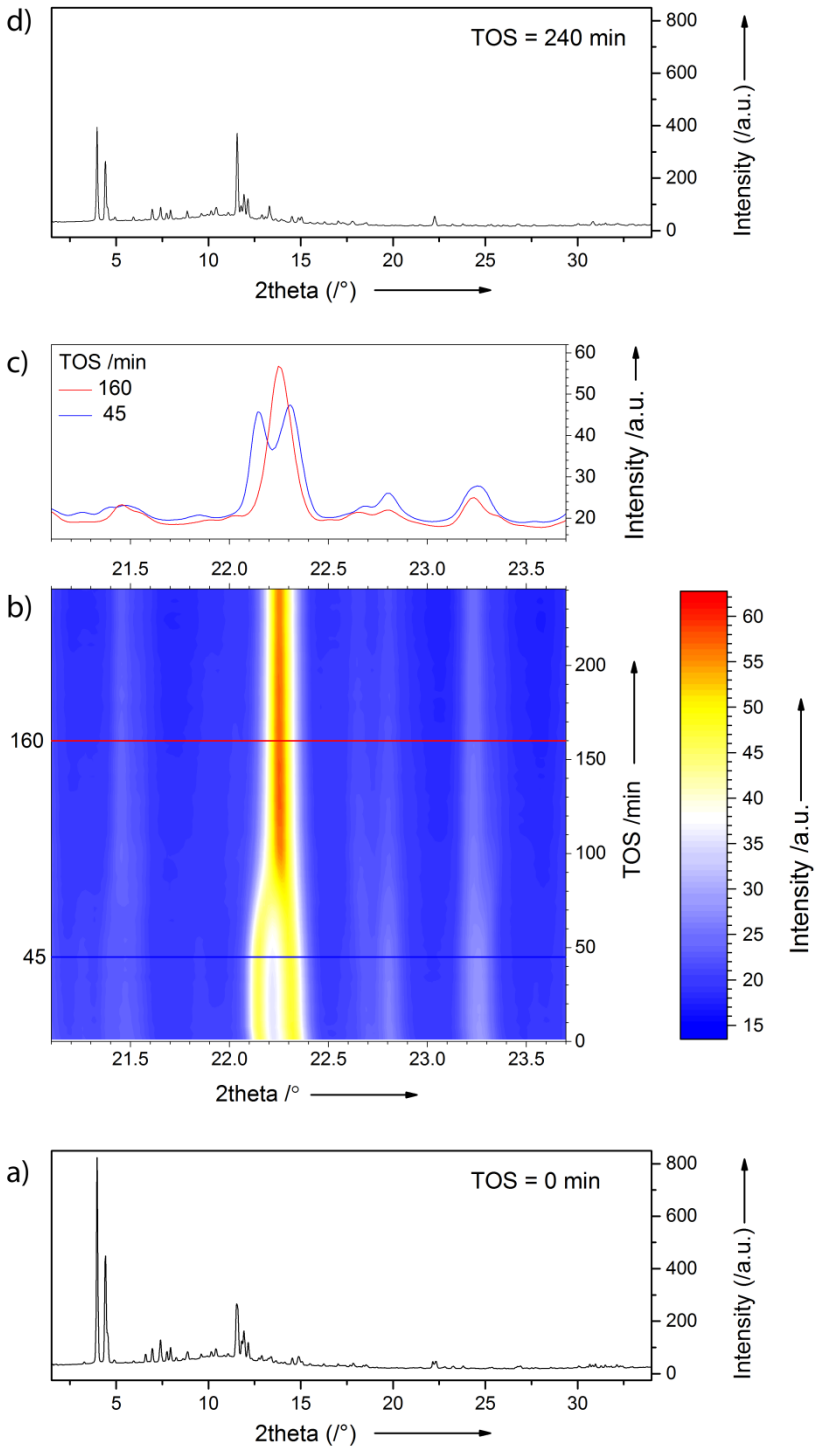


**Figure 2.** a) Diffractogram of the fresh H-ZSM-5 catalyst. b) Film plot showing the time-resolved diffraction patterns in the 21.1-23.7° 2θ range. c) Individual patterns at TOS 45 min (before the transition) and at 160 min. d) Diffractogram of the H-ZSM-5 catalyst at the end of the

MTH reaction. Film plot excerpt and diffractograms are taken by reactor layer 5 (center of the reactor). The wavelength in all cases is 0.7743 Å.

Figure 2a) contains the XRD pattern of the fresh H-ZSM-5 catalyst. (A small reflection at 3.3° matches the most intense peak of zeolite mordenite, a reasonable impurity for commercial MFI materials). The film plot shown in Figure 2b displays the evolution of the prominent doublet peak observed at 22.5 ° during reaction. The blue line in panel c) corresponds to the diffractogram of layer number 5 (center of the reactor) after 45 minutes on stream, whereas the red line shows the XRD pattern of the same area of the catalytic bed after 160 minutes of reaction. The film plot clearly shows the transformation of the doublet into a single peak with increasing degree of deactivation, as first observed for fully deactivated catalysts by Alvarez el at.[19]. The transformation is completed after 110 minutes and the new peak has higher intensity compared to the starting ones (Figures 2b and 2c). The full diffractogram of the catalyst after the MTH reaction is displayed in Figure 2d). Distinct intensity differences are observed. These are related to the presence of coke species in the micropores and will be commented on later.

The changes in the zeolite structure induced by the formation and accumulation of coke during deactivation are further evaluated by determining the difference between the lengths of the a- and b-axes of the unit cell in the different sections of the bed at increasing reaction time. For a further discussion of the choice of this exact descriptor, see the S.I. Panel a) Figure 3 shows the MS signals for the reactants; both MeOH (m/z = 31) and DME (m/z = 46) are considered as such, and for two representative products, alkenes (m/z = 41; a common and intense fragment for all C3+ alkenes) and aromatics (m/z = 91; tropylium ion). The MS signals show that the breakthrough of methanol occurs approximately after 120 minutes on stream. The time evolution of the (a-b) parameter for the different layers of the catalyst bed is shown in Figure 3b).

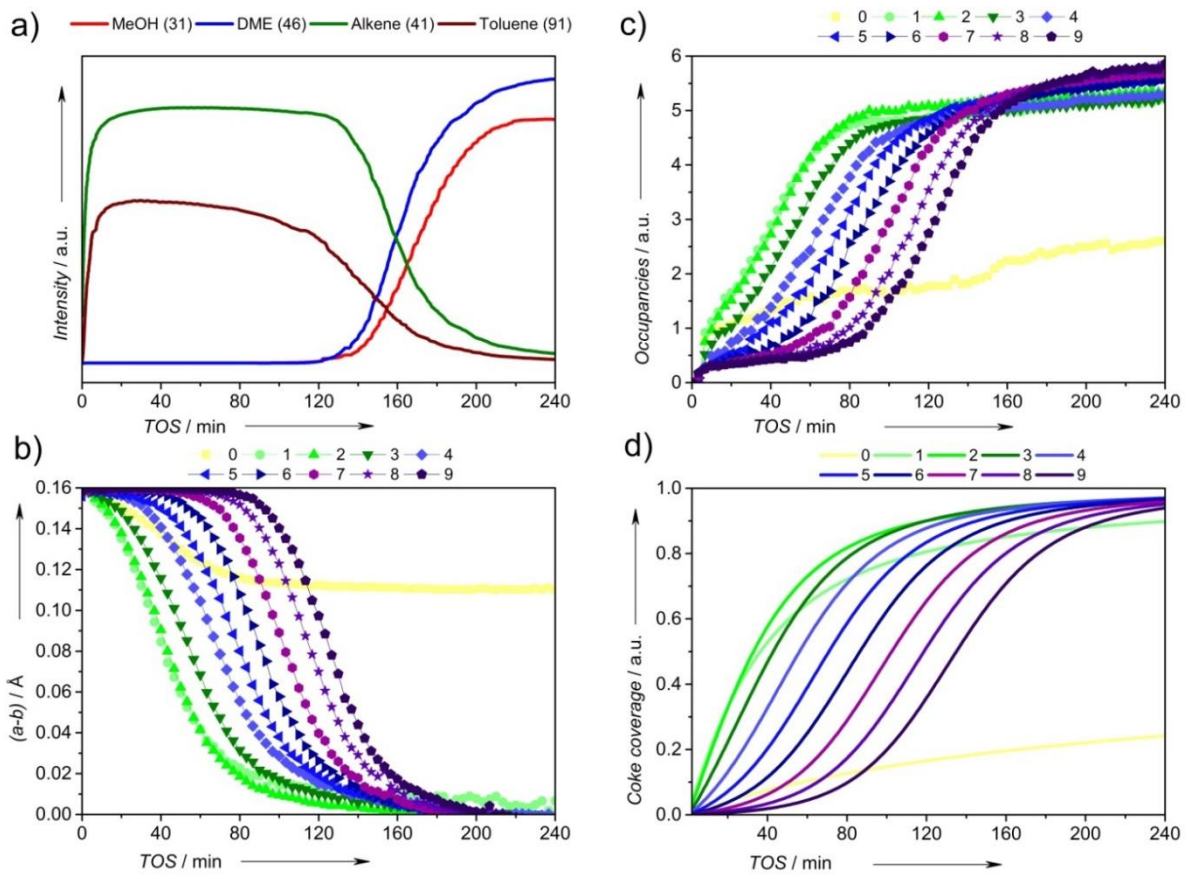


**Figure 3.** a) MS signals for MeOH, DME, alkenes and aromatics (multiplied by a factor of 10). b) The (a-b) parameter for the different layers of the catalytic reactor at increasing TOS. c) The total coke occupancies at increasing reaction times for the 10 reactor slices. d) Simulated coke coverage derived from the autocatalytic deactivation model.

Several observations can immediately be made. With the exception of the first layer (see below), the evolution of the (a-b) parameter strongly resembles the inverse S shaped curve characteristic for the typical deactivation profile during the conversion of methanol (see Figure 3a and the S.I.). Moreover, it is evident that the behavior of the (a-b) parameter is the same throughout the reactor, with the only difference that the decrease in the parameter is delayed for the layers located close to the outlet. For the final layer, it takes approximately 90 min until any change is seen. As detailed in the S.I., the breakthrough of methanol corresponds approximately

to a 50% reduction from starting to final value of (a-b) for this last layer. At complete deactivation, the (a-b) parameter has levelled off. Clearly, the (a-b) parameter is related to the activity, or more precisely to the degree of deactivation of the catalyst, and the reaction occurs in a cascade through the different layers of the bed. Finally, it is worth noting that in the reactor layer closest to the inlet (the area of the bed displaying a persistent white color in the photographs in Figure 1) the reduction of the (a-b) reaches a constant value of 0.11 Å after 80 minutes on stream. As mentioned, this behavior is believed to be due to the role of the first layer as the induction zone (see also below).[2]

Due to the high quality of the synchrotron data, the degree of deactivation can also be assessed by evaluating the coke occupancies based on residual electron density in the channels. Difference Fourier maps were used to assign the positions of dummy carbon atoms to each coke position in the framework channels, see S.I. Their individual occupancies were refined (with symmetry constraints) during subsequent cycles[14, 20-21]. This is related to the changes in intensity upon deactivation mentioned above. Panel c) of Figure 3 depicts the evolution of the total coke occupancy with reaction time for the different layers in the bed. The occupancies increase initially at the inlet, and remain negligible in subsequent layers for a certain period of time. The same cascade behavior is seen as for the (a-b) parameter, in line with the idea that coke is formed in a reaction zone that gradually progresses from inlet to outlet. The layers seem to level off on a similar coke occupancy value, suggesting that they reach a comparable degree of deactivation, i.e. full deactivation. However, for the first layer, a substantially lower final coke occupancy is reached, in line with the partial reduction seen also for the (a-b) parameter in the first layer. Clearly, the coke occupancies are inversely related to the (a-b) parameter. The evolution of the

(a-b) parameter, and thus the distortion of the unit cell, is thus strongly correlated to the accumulation of coke in the structure. In line with this, in a previous study we have employed DFT to show that the unit cell changes upon deactivation are related to the buildup of methylbenzene species at the channel intersections.[16]

To further extend our interpretation of the (a-b) parameter as a measure of the coking, we employed a kinetic model for the MTG reaction based on the dual cycle reaction mechanism, as presented by Janssens et al.[22] and outlined in reactions 1-4 below; see also S.I.

$$MeOH \xrightarrow{Alkene*} Alkene \qquad k_1 \qquad (1)$$

$$MeOH \xrightarrow{Aromatics*} Alkene \qquad k_2 \qquad (2)$$

$$Alkene* \rightarrow Aromatics* + Alkanes \qquad k_3 \qquad (3)$$

$$Aromatics* + MeOH \rightarrow Coke* \qquad k_4 \qquad (4)$$

Briefly, it is assumed that gas phase alkenes are formed indirectly when methanol reacts with adsorbed alkenes or aromatics (HCP species). Aromatics (and alkanes) are formally formed by disproportionation of alkenes, and coking involves the reaction between methanol and adsorbed aromatics. When applied as described in the S.I., the model produces the profiles shown in Figure 3d for the evolution of the coke concentration along the reactor bed with time. The model is able to reproduce the trends seen for both the occupancies and, inversely, for the (a-b) parameter, even for the very first layer. This essentially confirms that the behavior seen for the first layer is indeed related to accumulation of hydrocarbon pool species (adsorbed alkenes and aromatics in the model) which are required to facilitate the conversion.

In this work, we have followed the progressive deactivation of zeolite catalyst H-ZSM-5 during the conversion of methanol to gasoline. We observe the deactivation progressing in time

(time on stream) and space (along the axial reactor coordinate) with exceptional resolution. This is achieved by determining the difference in the lengths of the a- and b-unit cell axes, the (a-b) parameter, by Rietveld refinement of X-ray diffraction data. We further show that this parameter is related to amount of coke built up by comparison to the effluent composition, to the occupancies of coke species, and to a kinetic model taking the mechanisms of reaction and coke formation into account. Clearly, the changes seen with XRD are related to internal coke species. However, this does not allow us to draw definitive conclusions regarding the roles of internal and external coke. Provided there is some form of relationship between the amount of internal and external coke, a similar development would be observed. An interesting objective for further work would be to shed light on this, possibly by investigating other reactions that display different sensitivities to different types of coke, and/or to study materials with larger external surface areas (e.g. hierarchical materials). It is demonstrated that the low degree of coking nearest the reactor inlet seen here and elsewhere [4, 8, 16] is due to a kinetically slow buildup of aromatic hydrocarbon pool species. This work provides a proof of principle for operando monitoring of the deactivation of H-ZSM-5. A logical extension would be to apply this approach to a larger chemical reactor and/or to shaped catalyst objects as used in industrial systems. Moving in the other size direction, it would also be possible to track deactivation gradients across H-ZSM-5 aggregates or even within single crystallites.

## Experimental Methods

For the catalytic reactions, H-ZSM-5-MFI-27 was pressed into pellets, crushed and sieved to a size between 212-250 μm. Approximately 1 mg of catalyst was loaded on a quartz capillary reactor of 0.5 mm O.D. and 0.49 mm I.D. Reaction gases (argon, 20 % oxygen in argon, or argon

bubbled through methanol held at room temperature) were fed with a flow rate of 2.2 mL $min^{-1}$ (Weight Hourly Space Velocity, WHSV = 20 $g_{MeOH}$ $g_{catalyst}^{-1}$ $h^{-1}$). The reactor was heated with an Osram Sylvania heat blower. The temperature profile across an empty capillary reactor was measured inserting a thermocouple, and the temperature varied between 405 and 395 °C. Prior to reaction, the catalyst was activated at 500 °C for 1h using a stream of 20 % oxygen in argon. Then, the temperature was lowered to 400 °C, the reaction temperature.

A Pfeiffer Omnistar GSD 301 T3 Quadrapole mass spectrometer was coupled at the exhaust line of the flow cell (sample to instrument distance <30 cm) for mass spectrometry data acquisition during the activation and MTH reaction. The total acquisition and read out time of each of the acquired mass spectrum was <0.8 s.

Powder X-ray Diffraction data (PXRD) data were collected at Swiss-Norwegian beamline (station BM01A/BM01) of the European Synchrotron Facility (ESRF) with a wavelength of 0.7743 Å, using a Dectris Pilatus 2M photon counting pixel area detector[23]. The capillary reactor was mounted on a Huber stage capable of translations in the *z* direction. A Huber goniometer head was used for alignment and phi rotations. During data collection the reactor was moved across the beam where diffractograms were acquired in 10 different layers of the bed of fixed time and distance intervals. After completing a full scan of the capillary, the reactor was moved back with no data collection.

The data were azimuthally integrated to 2D powder patterns with the SNBL Bubble software[24]. with a 2θ range from 0 to 51°. The patterns were analyzed by parametric Rietveld refinement [25] using TOPAS[26] to extract the unit cell parameters (orthorhombic cell; Pnma space group), framework atom positions and the coke occupancy for each individual coke position in the MFI framework as a function of time-on-stream.

ASSOCIATED CONTENT

Supplementary Information accompanies this paper.

ACKNOWLEDGMENT

Authors acknowledge ESRF for granting beamtime at SNBL (BM01). This publication is part of the European Industrial Doctorate Project ‘‘ZeoMorph” (Grant Agreement No. 606965).

REFERENCES

(1) Stöcker, M. Methanol-to-Hydrocarbons: Catalytic Materials and Their Behavior. *Microporous Mesoporous Mater.* **1999,** *29*, 3-48.

(2) Olsbye, U.; Svelle, S.; Bjørgen, M.; Beato, P.; Janssens, T. V. W.; Joensen, F.; Bordiga, S.; Lillerud, K. P. Conversion of Methanol to Hydrocarbons: How Zeolite Cavity and Pore Size Controls Product Selectivity. *Angew. Chem., Int. Ed.* **2012,** *51*, 5810-5831.

(3) Olsbye, U.; Svelle, S.; Lillerud, K. P.; Wei, Z. H.; Chen, Y. Y.; Li, J. F.; Wang, J. G.; Fan, W. B. The Formation and Degradation of Active Species During Methanol Conversion over Protonated Zeotype Catalysts. *Chem. Soc. Rev.* **2015,** *44*, 7155-7176.

(4) Schulz, H. “Coking” of Zeolites During Methanol Conversion: Basic Reactions of the Mto-, Mtp- and Mtg Processes. *Catal. Today.* **2010,** *154*, 183-194.

(5) Cobb, J.; Corporation, N. Z. S. F. *New Zealand Synfuel the Story of the World's First Natural Gas to Gasoline Plant*. Auckland, NZ: **1985**.

(6) Haw, J. F.; Marcus, D. M. Well-Defined (Supra)Molecular Structures in Zeolite Methanol-to-Olefin Catalysis. *Top Catal* **2005,** *34*, 41-48.

(7) Rojo-Gama, D.; Etemadi, S.; Kirby, E.; Lillerud, K. P.; Beato, P.; Svelle, S.; Olsbye, U. Time- and Space-Resolved Study of the Methanol to Hydrocarbons (Mth) Reaction - Influence of Zeolite Topology on Axial Deactivation Patterns. *Faraday Discuss.* **2017,** *197*, 421-446.

(8) Bleken, F. L.; Barbera, K.; Bonino, F.; Olsbye, U.; Lillerud, K. P.; Bordiga, S.; Beato, P.; Janssens, T. V. W.; Svelle, S. Catalyst Deactivation by Coke Formation in Microporous and Desilicated Zeolite H-Zsm-5 During the Conversion of Methanol to Hydrocarbons. *J. Catal.* **2013,** *307*, 62-73.

(9) Müller, S.; Liu, Y.; Vishnuvarthan, M.; Sun, X.; van Veen, A. C.; Haller, G. L.; Sanchez-Sanchez, M.; Lercher, J. A. Coke Formation and Deactivation Pathways on H-Zsm-5 in the Conversion of Methanol to Olefins. *J. Catal.* **2015,** *325*, 48-59.

(10) O'Brien, M. G.; Beale, A. M.; Jacques, S. D.; Di Michiel, M.; Weckhuysen, B. M. Spatiotemporal Multitechnique Imaging of a Catalytic Solid in Action: Phase Variation and Volatilization During Molybdenum Oxide Reduction. *ChemCatChem* **2009,** *1*, 99-102.

(11) Beale, A. M.; Jacques, S. D.; Gibson, E. K.; Di Michiel, M. Progress Towards Five Dimensional Diffraction Imaging of Functional Materials under Process Conditions. *Coord. Chem. Rev.* **2014,** *277*, 208-223.

(12) Wragg, D. S.; Johnsen, R. E.; Balasundaram, M.; Norby, P.; Fjellvåg, H.; Grønvold, A.; Fuglerud, T.; Hafizovic, J.; Vistad, Ø. B.; Akporiaye, D. Sapo-34 Methanol-to-Olefin Catalysts under Working Conditions: A Combined in Situ Powder X-Ray Diffraction, Mass Spectrometry and Raman Study. *J. Catal.* **2009,** *268*, 290-296.

(13) Wragg, D. S.; O'Brien, M. G.; Bleken, F. L.; Di Michiel, M.; Olsbye, U.; Fjellvag, H. Watching the Methanol-to-Olefin Process with Time- and Space-Resolved High-Energy Operando X-Ray Diffraction. *Angew. Chem., Int. Ed.* **2012,** *51*, 7956-7959.

(14) Wragg, D. S.; Bleken, F. L.; O'Brien, M. G.; Di Michiel, M.; Fjellvåg, H.; Olsbye, U. The Fast Z-Scan Method for Studying Working Catalytic Reactors with High Energy X-Ray Diffraction: Zsm-5 in the Methanol to Gasoline Process. *Phys. Chem. Chem. Phys.* **2013,** *15*, 8662-8671.

(15) del Campo, P.; Slawinski, W. A.; Henry, R.; Erichsen, M. W.; Svelle, S.; Beato, P.; Wragg, D.; Olsbye, U. Time- and Space-Resolved High Energy Operando X-Ray Diffraction for Monitoring the Methanol to Hydrocarbons Reaction over H-Zsm-22 Zeolite Catalyst in Different Conditions. *Surf. Sci.* **2016,** *648*, 141-149.

(16) Rojo-Gama, D.; Nielsen, M.; Wragg, D. S.; Dyballa, M.; Holzinger, J.; Falsig, H.; Lundegaard, L. F.; Beato, P.; Brogaard, R. Y.; Lillerud, K. P.; Olsbye, U.; Svelle, S. A Straightforward Descriptor for the Deactivation of Zeolite Catalyst H-Zsm-5. *ACS Catal.* **2017,** *7*, 8235-8246.

(17) Kaarsholm, M.; Joensen, F.; Nerlov, J.; Cenni, R.; Chaouki, J.; Patience, G. S. Phosphorous Modified Zsm-5: Deactivation and Product Distribution for Mto. *Chem. Eng. Sci.* **2007,** *62*, 5527-5532.

(18) Bleken, F. L.; Janssens, T. V. W.; Svelle, S.; Olsbye, U. Product Yield in Methanol Conversion over Zsm-5 Is Predominantly Independent of Coke Content. *Microporous Mesoporous Mater.* **2012,** *164*, 190-198.

(19) Alvarez, A. G.; Viturro, H.; Bonetto, R. D. Structural Changes on Deactivation of Zsm-5. A Study by X-Ray Powder Diffraction. *Mater. Chem. Phys.* **1992,** *32*, 135-140.

(20) Wragg, D. S.; Akporiaye, D.; Fjellvåg, H. Direct Observation of Catalyst Behaviour under Real Working Conditions with X-Ray Diffraction: Comparing Sapo-18 and Sapo-34 Methanol to Olefin Catalysts. *J. Catal.* **2011,** *279*, 397-402.

(21) Kalantzopoulos, G. N.; Lundvall, F.; Lind, A.; Arstad, B.; Chernyshov, D.; Fjellvåg, H.; Wragg, D. S. Sapo-37 Microporous Catalysts: Revealing the Structural Transformations During Template Removal. *Catal. Struct. React.* **2017,** *3*, 79-88.

(22) Janssens, T. V. W.; Svelle, S.; Olsbye, U. Kinetic Modeling of Deactivation Profiles in the Methanol-to-Hydrocarbons (Mth) Reaction: A Combined Autocatalytic–Hydrocarbon Pool Approach. *J. Catal.* **2013,** *308*, 122-130.

(23) Dyadkin, V.; Pattison, P.; Dmitriev, V.; Chernyshov, D. A New Multipurpose Diffractometer Pilatus@ Snbl. *J. Synchrotron Radiat.* **2016,** *23*, 825-829.

(24) Müller, S.; Liu, Y.; Kirchberger, F. M.; Tonigold, M.; Sanchez-Sanchez, M.; Lercher, J. A. Hydrogen Transfer Pathways During Zeolite Catalyzed Methanol Conversion to Hydrocarbons. *J. Am. Chem. Soc.* **2016,** *138*, 15994-16003.

(25) Stinton, G. W.; Evans, J. S. Parametric Rietveld Refinement. *J. Appl. Crystallogr.* **2007,** *40*, 87-95.

(26) TOPAS 5.0, B. A., 2012. Available from: http://;www.topas-academic.net/. (Access day: 20/12/2017)